Internal calibration of the LUX detector using tritiated methane

D.S. Akerib,[1] H.M. Araújo,[2] X. Bai,[3] A.J. Bailey,[2] J. Balajthy,[4] E. Bernard,[5] A. Bernstein,[6] A. Bradley,[1]
D. Byram,[7] S.B. Cahn,[5] M.C. Carmona-Benitez,[8] C. Chan,[9] J.J. Chapman,[9] A.A. Chiller,[7] C. Chiller,[7]
T. Coffey,[1] A. Currie,[2] L. de Viveiros,[10] A. Dobi,[4] J. Dobson,[11] E. Druszkiewicz,[12] B. Edwards,[5] C.H. Faham,[13]
S. Fiorucci,[9] C. Flores,[14] R.J. Gaitskell,[9] V.M. Gehman,[13] C. Ghag,[15] K.R. Gibson,[1] M.G.D. Gilchriese,[13] C. Hall,[4]
S.A. Hertel,[5] M. Horn,[5] D.Q. Huang,[9] M. Ihm,[16] R.G. Jacobsen,[16] K. Kazkaz,[6] R. Knoche,[4] N.A. Larsen,[5]
C. Lee,[1] A. Lindote,[10] M.I. Lopes,[10] D.C. Malling,[9] R. Mannino,[17] D.N. McKinsey,[5] D.-M. Mei,[7] J. Mock,[14]
M. Moongweluwan,[12] J. Morad,[14] A.St.J. Murphy,[11] C. Nehrkorn,[8] H. Nelson,[8] F. Neves,[10] R.A. Ott,[14] M. Pangilinan,[9]
P.D. Parker,[5] E.K. Pease,[5] K. Pech,[1] P. Phelps,[1] L. Reichhart,[15] T. Shutt,[1] C. Silva,[10] V.N. Solovov,[10] P. Sorensen,[6]
K. O'Sullivan,[5] T.J. Sumner,[2] M. Szydagis,[14] D. Taylor,[18] B. Tennyson,[5] D.R. Tiedt,[3] M. Tripathi,[14] S. Uvarov,[14]
J.R. Verbus,[9] N. Walsh,[14] R. Webb,[17] J.T. White,[17] M.S. Witherell,[8] F.L.H. Wolfs,[12] M. Woods,[14] and C. Zhang[7]

[1]*Case Western Reserve University, Dept. of Physics, 10900 Euclid Ave, Cleveland OH 44106, USA*
[2]*Imperial College London, High Energy Physics, Blackett Laboratory, London SW7 2BZ, UK*
[3]*South Dakota School of Mines and Technology, 501 East St Joseph St., Rapid City SD 57701, USA*
[4]*University of Maryland, Dept. of Physics, College Park MD 20742, USA*
[5]*Yale University, Dept. of Physics, 217 Prospect St., New Haven CT 06511, USA*
[6]*Lawrence Livermore National Laboratory, 7000 East Ave., Livermore CA 94551, USA*
[7]*University of South Dakota, Dept. of Physics, 414E Clark St., Vermillion SD 57069, USA*
[8]*University of California Santa Barbara, Dept. of Physics, Santa Barbara, CA, USA*
[9]*Brown University, Dept. of Physics, 182 Hope St., Providence RI 02912, USA*
[10]*LIP-Coimbra, Department of Physics, University of Coimbra, Rua Larga, 3004-516 Coimbra, Portugal*
[11]*SUPA, School of Physics and Astronomy, University of Edinburgh, Edinburgh, EH9 3JZ, UK*
[12]*University of Rochester, Dept. of Physics and Astronomy, Rochester NY 14627, USA*
[13]*Lawrence Berkeley National Laboratory, 1 Cyclotron Rd., Berkeley, CA 94720, USA*
[14]*University of California Davis, Dept. of Physics, One Shields Ave., Davis CA 95616, USA*
[15]*Department of Physics and Astronomy, University College London, Gower Street, London WC1E 6BT, UK*
[16]*University of California Berkeley, Department of Physics, Berkeley, CA 94720, USA*
[17]*Texas A & M University, Dept. of Physics, College Station TX 77843, USA*
[18]*South Dakota Science and Technology Authority, Sanford Underground Research Facility, Lead, SD 57754, USA*

We describe the development, deployment, and exploitation of a tritium calibration source for the LUX dark matter experiment. The source is useful for calibrating the electron recoil backgrounds over the full volume of the detector, and for characterizing the behavior of the LUX TPC. We report on the LUX electron recoil discrimination factor, the detector threshold, and on the detector physics of liquid xenon at the LUX electric field value of 181 V/cm.

I. Introduction

The LUX collaboration recently reported results from its first underground science run, placing new constraints on WIMP dark matter with masses between 6 GeV and 1 TeV[**?**]. LUX is a large dual-phase liquid xenon (LXe) time projection chamber (TPC) with an active mass of ??270?? kg. The primary scintillation light from particle interactions (S1) is collected by two arrays of photomultiplier tubes (PMTs) at the top and bottom of the detector, and the charge signal is converted to light via secondary scintillation at the anode (S2).

Measurement of both S1 and S2 allows the event to be located in all three dimensions, and allows discrimination between nuclear recoil (NR) events and electron recoil (ER) events via the ratio (S2/S1).

One of the primary advantages of the liquid TPC technology is its high efficiency for the rejection of external gamma backgrounds via self-shielding. On the other hand, self-shielding also reduces the effectiveness of external gamma calibration sources such as ^{137}Cs or ^{228}Th , particularly in the center of the detector and at the low energies relevant for dark matter searches. In the case of LUX, external gamma sources are unable to produce a useful rate of ER calibration events in the

fiducial region.

To address this issue, internal calibration sources that can be dissolved into the liquid xenon and thereby defeat its self-shielding have been developed[**?**]. LUX has deployed two such internal calibration sources; the first based upon ^{83m}Kr , and the second based upon tritium (^{3}H). ^{83m}Kr is a source of two internal conversion electrons at energies of 9.4 keVee and 32.1 keVee separated in time by an intermediate state with a half life of 154 ns. Because it produces two lines in the energy spectrum, ^{83m}Kr is suitable for tracking the spatial and time dependence of the S1 and S2 signals. However, because both ^{83m}Kr electrons are above the energy range of interest for dark matter (1.3 - 8 levee), and because the S2 signals from the two electrons generally overlap with each other in the detector, ^{83m}Kr is less useful for constraining the electron recoil (ER) band of the S2/S1 discriminant.

In this article we describe the development and use of the LUX tritium source, which plays a complementary role to the ^{83m}Kr source. Unlike ^{83m}Kr , tritium is a single-beta emitter, with a Q value of 18.6 keVee. Its spectral maximum is at 2.5 keVee, and 75% of its beta decays are below 8 keVee. This allows the detector's ER band to be precisely characterized throughout the full volume of the detector and allows the threshold response of the detector to be studied.

Unlike ^{83m}Kr , however, tritium is long-lived, with a half-life of 12.3 years (compared to 1.8 hours for ^{83m}Kr), so the tritium must be removed from the liquid xenon by purification. Secondly, tritium must be introduced into the detector in a manner which will not impair the charge or light collection properties of the detector. This is less of a concern with ^{83m}Kr , both because krypton is a noble element, and because spectator electronegative impurities intrinsic to the source may be removed by passing the krypton through the LUX getter prior to entering the detector. Tritium, on the other hand, is removed by the getter, and must therefore be introduced downstream.

Tritiated methane (CH$_3$T) was chosen as the appropriate host molecule to deliver the activity into LUX. Methane has several desirable chemical and physical properties compared to T$_2$: first, its diffusion constant (D) times solubility (K) at room temperature is ten times smaller in common LUX materials such as teflon (PTFE) and polyethylene (PE)[**?**], mitigating the problem of back-diffusion of activity into the liquid xenon after purification; it is chemically inert, so it is not expected to adhere to surfaces (as the T$_2$ molecule is known to do), and it is consistent with maintaining good charge transport in liquid xenon.

In developing and deploying the source, our purification goal was that any residual activity that remained due to back-diffusion from plastics or from inefficient purification should be no more than 0.33 μBq, which is 5% of the LUX ER background rate design goal for a 30,000 kg·days exposure. We desired to collect a LUX calibration dataset of ∼15,000 tritium events, roughly a factor of 100 larger than the number of expected ER background events in LUX.

This article is organized as follows. In Section **??**, we describe the bench-top purification tests and calculations that we employed to verify the suitability of the tritiated methane source for injection and removal from LUX. In Section **??** we describe the analysis of the tritium decay data collected by LUX and its implications for our WIMP dark matter search.

II. Development of the Calibration Source

1. Tritiated Methane Removal

The removal efficiency of zirconium getters for methane in xenon had previously been studied at the University of Maryland. It was found that greater than 99.99% of natural methane can be removed in a single pass through a zirconium getter. [1] Tritiated methane is chemically identical to natural methane, so it follows that similar removal efficiencies should be expected for CH$_3$T. To verify this a small scale tritiated methane injection system was integrated into a liquid xenon system at the University of Maryland. This system used a SAES MC1-905F methane purifier placed in series immediately after the CH$_3$T source bottle to prevent non-methane species of tritium from entering the plumbing. Over 68,000 Bq of observed CH$_3$T activity was injected into this small scale system and a removal efficiency of over 99.99% for tritiated methane in xenon was confirmed.

2. Out Gassing of Tritiated Methane from Plastics

An accurate model of a tritiated methane injection into LUX must account for out gassing of CH$_3$T from plastics such as polyethylene and teflon. Using data from the liquid xenon experiments at the University of Maryland we numerically modeled the purification and residual diffusion of CH$_3$T in the detector. Using Duhamel's priciple, the analytic solution to Fick's second law on a half-infite line is

$$\phi(x,t) = KC_{out} - \int_0^t erf(\frac{x}{\sqrt{4D(t-\tau)}})KC'_{out}(\tau)d\tau - KC_{out}(0)erf(\frac{x}{\sqrt{4Dt}}),$$
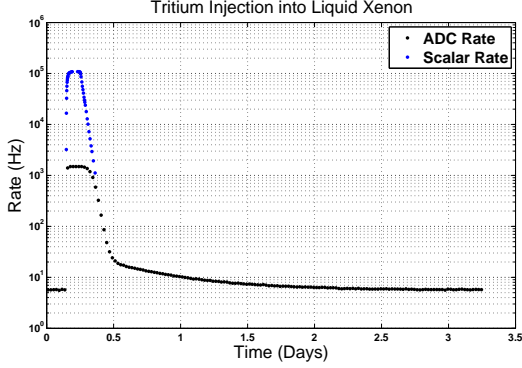
FIG. 1: A time histogram of the event rate during a tritium injection into our small scale detector. The event rate greatly exceeded the limits of our ADC (black data points), so a analog scalar was used to count the true event rate (blue data points).

where K is the solubility of the material, D is the diffusion constant, and C_{out} is the outside concentration of the material. [?] For the out gassing process we are only able to detect the flux of material out of the plastic. This is given by Fick's first law evaluated at $x = 0$,

$$J_{out}(t) = -K\sqrt{\frac{D}{\pi}}\left(\int_0^t \frac{\dot{C}_{out}(\tau)}{\sqrt{t - \tau}}d\tau + \frac{C_{out}(t)}{\sqrt{t}}\right),$$

where the sign has been flipped since the flux of material is outward. We see that it is no longer possible to evaluate K and D separately, since the diffusion in and out of the plastic is completely determined by the time-dependent concentration outside of the plastic. To simplify our model, we define a new constant

$$G = K\sqrt{\frac{D}{\pi}}.$$

By fitting the integral of the flux out of the plastic over time to out gassing data collected in Maryland's liquid xenon system we constrain $G \leq 0.01 \frac{cm}{\sqrt{day}}$.

With a constraint on G taken from the analytic solution to Fick's second law, we turn to numerical simulation to answer the question of how much initial CH_3T activity to inject into LUX to meet our calibration conditions. Several assumptions are made to simplify the numerical model. First, we approximate the diffusion into plastic as being a one dimensional

process. Since the plastic in our detector at Maryland and in LUX can be approximated by a cylindrical shell, there is no dependence on the azimuthal or z coordinates. Since r is large compared to the thickness of the plastic shell, $\frac{\delta^2\phi}{\delta r^2} \gg \frac{1}{r}\frac{\delta\phi}{\delta r}$, so Fick's laws in a one dimensional approximation become

$$J = -D\frac{\delta\phi}{\delta r}\vec{r}$$

$$\frac{\delta\phi}{\delta t} = D\frac{\delta^2\phi}{\delta r^2}.$$

We assume the concentration of CH_3T in LUX is uniform throughout its volume, since the design of LUX creates currents which stir the liquid xenon. With perfect mixing the effect of the purifier can be modeled by adding an exponential time dependence to the outer volume. The time constant of this decay has an upper limit equal to the time it takes xenon to recirculate through the LUX detector, although in reality the mass transport from diffusion in the liquid and gaseous xenon decreases this time constant.

We use a simple implementation of the first order Euler method for our numerical simulations. The diffusion is simulated by setting the concentration at the boundary of the piece equal to KC_{out}, where C_{out} is the concentration of CH_3T in the xenon. This concentration is dependent on time according to

$$\frac{\delta C_{out}}{\delta t} = J_{out}\frac{A_{plastic}}{V_{xenon}} - \frac{C_{out}}{\tau},$$

where $A_{plastic}$ is the surface area of the plastic cylinder, V_{xenon} is the total volume of xenon in the fiducial region, and τ is the time it takes for one full purification cycle. The first term on the right of this equation models out gassing of CH_3T from the plastic cylinder, while the second term models removal of CH_3T through purification. Using the first order Euler method, we arrive at an expression for C_{out} given by

$$C_{j+1} = C_j + \Delta t[(J_{1,j} - J_{N_x,j})\frac{A_{plastic}}{V_{xenon}} - \frac{C_j}{\tau}].$$

The initial concentration is defined by dividing the desired injection activity by the volume of the fiducial region. We choose $D = 2.3 \times 10^{-9} \frac{cm^2}{sec}$ so that the half-infinite boundary conditions in our diffusion model is valid, and combine this with our allowed range of values for G to extract a value for K. We use this model to predict the total number of calibration events as well as the time required to return to $<5\%$ of the nominal background rate for any CH_3T injection into LUX.
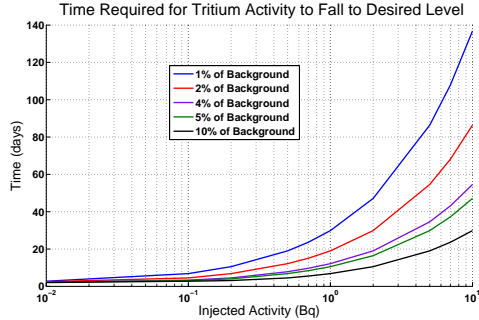
FIG. 2: Time required to remove CH_3T from LUX after various injections.

III. Implementation of the Calibration Source

1. Injection System Hardware

The setup of our triated methane calibration technique can be separated into three parts: the tritiated methane source bottle, the injection system, and the zirconium getter.

The tritiated methane source bottle for our calibration technique consists of a 2250 cc stainless steel bottle which is filled with a mixture of tritiated methane and purified xenon. The purpose of this xenon is to serve as a carrier gas for the tritiated methane. The total activity in the source bottle is set by mixing tritiated methane from a reservoir into the source bottle via volume sharing.

The injection system for our tritiated methane calibration technique consists of a series of expansion volumes which are used to fine tune the amount of CH_3T that is injected. Once the CH_3T source bottle is opened it flows through a methane gas purifier (SAES MC1-905F) to remove any non-methane species of tritium, such as bare tritium. The expansion volumes are then filled with tritiated methane from the source bottle, and the flow of xenon in the gas system is diverted through the expansion volumes to sweep the CH_3T into the detector. A pump out port allows the expansion volumes to be evacuated in preparation for each use of the injection system.

The LUX gas system uses a hot zirconium getter (SAES-PS4MT15R1) located upstream of the CH_3T injection system to remove CH_3T from the xenon after passing through the detector.
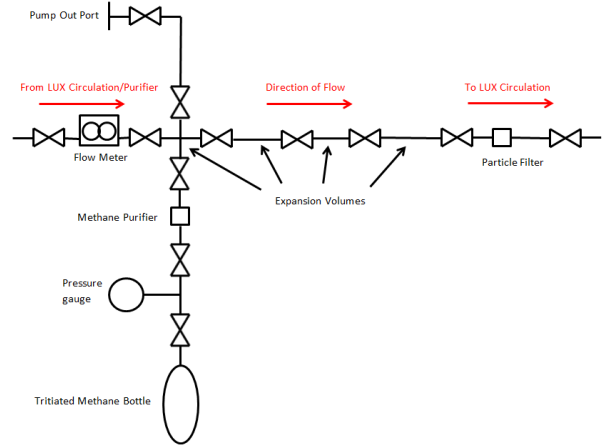

FIG. 3: Plumbing diagram of the tritium injection system for LUX.

2. Natural Methane Injection

Prior to injecting tritiated methane into the LUX detector 0.02 grams of natural methane were injected into LUX using the injection system. Purity samples from the detector were collected over the next few days, and a purification time constant of 5.90 ± 0.07 hours was determined using data collected with the LUX gas sampling system.

3. Tritiated Methane Injection

To confirm the purification model established by the natural methane injection a small amount of tritiated methane was injected into LUX the following week. An absolute activity of 20 mBq of tritiated methane was injected with the getter in purify mode. Thus as soon as the CH3T passed through the detector it was immediately removed. A purification time constant of 6.7 hours was observed, consistent with the natural methane purification rate measured by the sampling system. After a day of circulating through the getter the tritium decay had fallen below detectable amounts confirming the effective removal of the tritiated methane with the getter.

After confirming our purification model a larger injection of 800 mBq was performed. This second injection produced 20,000 beta decay events in the LUX detector before being completely removed, 5000 of those events could be used the calibrate the ER band in the WIMP search region of 0-30 Phe
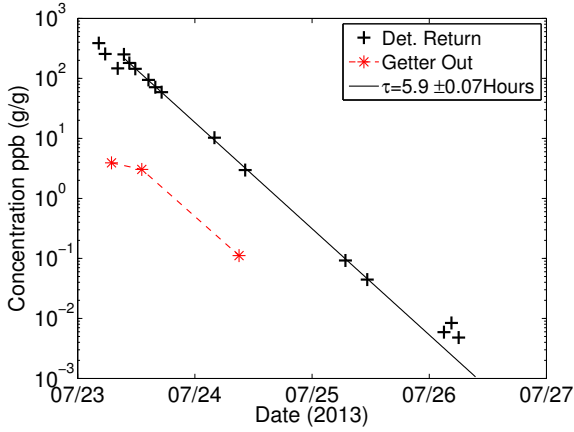
FIG. 4: Removal of natural methane observed by the integrated xenon sampling system prior to the tritiated methane injections. The red points indicate xenon gas measurements at the getter outlet, we find a 97% one pass removal efficiency at a flow rate of 25 SLPM. 1 10^{-3} ppb (g/g) is the limit of detection for methane using the LUX gas sampling system.

(pulse area in photo electrons). Figure 6 shows the two tritium injections and the subsequent CH3T purification. The rate of tritiated methane removal was consistent with the previous two injections $1/10^5$.

IV. Results from the Tritiated Methane Calibration

1. Mixing of Tritiated Methane in Liquid Xenon

Tritium events appear uniformly distributed in the liquid volume several minutes after injecting the tritiated methane inline with the xenon gas circulation path. Figure 5 shows the XY and Z distribution of tritium events thirty minutes after an injection. The events shown cover the region from the gate to the cathode and radially out to the edge of the detector. An additional cut requiring that the event be between $\pm 3\sigma$ of the ER mean was made to diregard residual alpha events from the walls and cathode, the event rate consisted overwhelmingly of tritium events. The tritiated methane dispersed uniformly throughout the liquid xenon illuminating all regions on the detector.
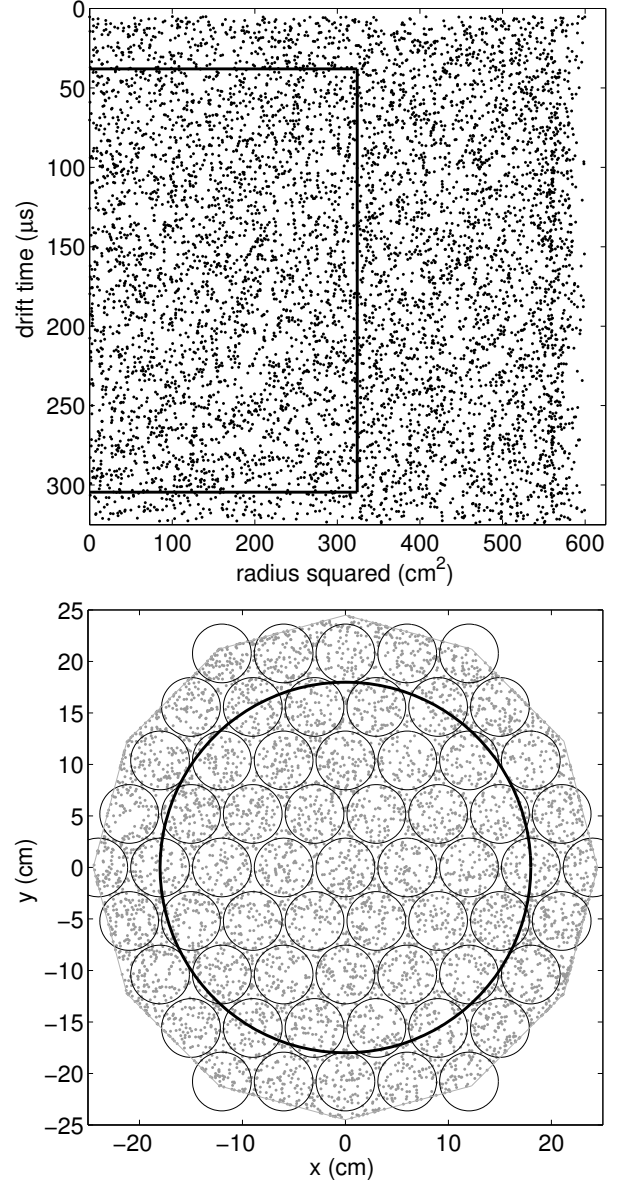

FIG. 5: Left: The distribution of tritium events vs. detector radius squared. The solid black line represents the fiducial volume. Right: The distribution of tritium events vs. XY in the region between the gate and the cathode. The solid black line represents the fiducial volume and the black circles represent the locations of PMTs (photo multiplier tubes).
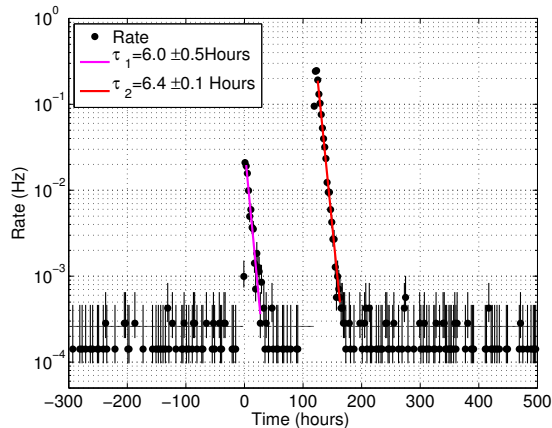
FIG. 6: Left: Rate of single scatter events with S1 below 150 Phe in the fiducial volume. 150 Phe in S1 is about 18.6 keVee, the endpoint to the tritium beta spectrum. The magenta and red curves are fits to the first and second tritium injection's removal rate. Right: The rate of single scatter events with S1 below 150 for the whole detector volume. Note the removal of tritiated methane is consistent with the natural methane removal rate measured independently.

2. Definition of Electronic Recoil Band and Comparison with NEST Model

Using the tritium source we calibrated the electronic recoil band in the fiducial volume of the LUX detector to unprecedented accuracy. Figure 7 shows the mean of the ER band along with the 10-90% confidence bounds ($\pm 1.28\sigma$) obtained from the beta decay of tritium at a drift field of 180 V/cm. The results of the leakage fraction at 50% NR acceptance per each 1 Phe bins in S1 are shown in 8. The nuclear recoil band, in red, is defined by the NEST model along with AmBe and ^{252}Cf calibrations. Methane will not quench xenon scintillation [[2]] shows that if methane is introduced into the xenon at a relative concentration of a few percent, then the amount of scintillation produced by the mixture is reduced by a factor of two compared to pure xenon. But for our application we require a methane concentration of only one part in 10^{15}, and therefore our methane injection will not have any negative effects on scintillation production and transport.

WIMPs primarily interact with the atomic nuclei xenon atoms in LUX resulting in nuclear recoils whereas the vast ma-jority of residual radioactivity within the detector are gammas which result in electronic recoils. Thus, knowing the separation of the ER from the NR band allows for a measure of the background rejection of a liquid xenon WIMP search experiment. We define the measure of background rejection as leakage fraction, reported here as the fraction of events in the ER band that spill into the lower half of the NR band. Over 115,000 tritium decays were used for the ER band calibration, between 1-50 Phe in S1 (1-8 keVee), and were found using standard WIMP search cuts within the fiducial volume. A figure of merit for ER and NR discrimination is the leakage fraction defined as the number of tritium events populating the lower half of the NR band are compared to the total number of tritium events in the selected energy range. Figure 8 shows the leakage fraction per 1 Phe bins in S1. The mean leakage fraction in the region used for the LUX 2013 PRL results, between 1-30 Phe (1-5 keVee) in the fiducial, was found to be 0.42% $\pm$ 0.02%, see Figure 8. In the 40 hour time window in which the data was acquired less than three out of 115,000 events are expected to be non tritium [BG paper reference]. The NR band used is from NEST version 0.98 and is vetted with AmBe, ^{252}Cf and DD neutron generator calibrations.
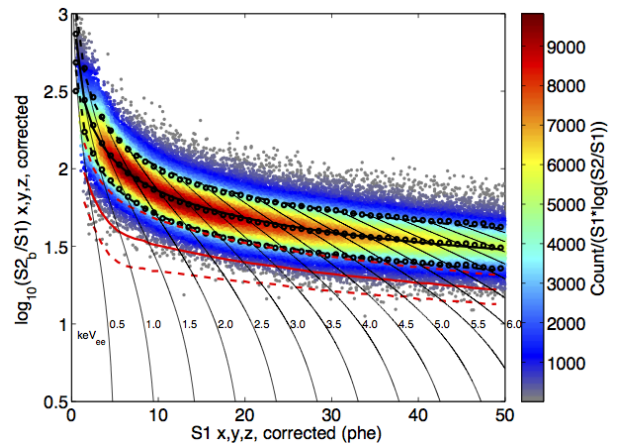

FIG. 7: Discrimination vs. S1 using over 115,000 tritium beta decays between 1 and 50 Phe in S1 (about $1 - 8\text{keV}_{ee}$). On average from 1 to 30 Phe the discrimination is 99.58%, defined by the fraction of events of events below the mean of the nuclear recoil band. The red band represents the NEST nuclear recoil band (version 0.98) vetted with an AmBe, ^{252}Cf and DD neutron generator calibration.
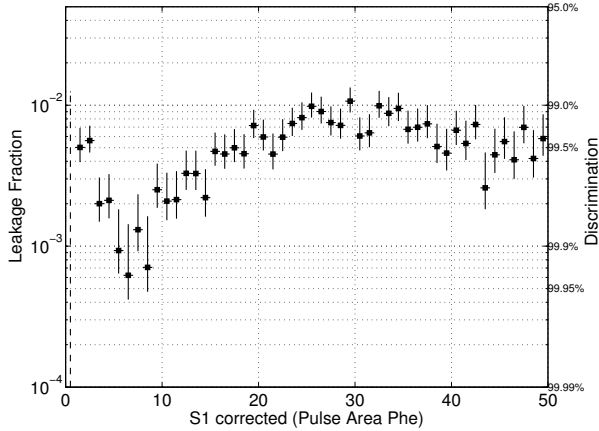
FIG. 8: Discrimination vs. S1 using over 115,000 tritium beta decays between 1 and 50 Phe in S1 (about $1 - 8\text{keV}_{ee}$). On average from 1 to 30 Phe the discrimination is 99.58%, defined by the fraction of events of events below the mean of the nuclear recoil band. The red band represents the NEST nuclear recoil band (version 4c) vetted with an AmBe, ^{252}Cf and DD neutron generator calibration.

V. All the things we can do with Tritium

- Define the ER band.

- Binned leakage fraction, and potentially optimize for spacial dependent leakage fraction in XYZ plane.

- S1, S2 threshold. (Energy is a bit convoluted let's not go there). Requires NEST

- Combined energy calibration to about 0.5 keVee. Requires NEST

- Light Yield, Charge Yield. Requires some trivial smearing model, 10% effect.

- Fano-like factor vs. energy. Requires some trivial smearing model, sub 2% effect.

- Fiducial mass calculation, optimized for low energy S2s making it more WIMP like.

- g1 and g2 calculation by competing tritium spectrum with NEST, or multiple E fields

- ER band Gaussianity.

- ... anything else?

VI. Summary

We have presented our new technique for injecting and removing CH_3T as an internal calibration source in detectors which utilize liquid and gas phase noble gases. We discussed the assembly of our CH_3T calibration system, motivated by gas and liquid phase R&D experiments at the University of Maryland. We have used data from the LUX detector to show that our system can safely inject CH_3T for the purpose of internal calibration.

[1] Study of a zirconium getter for purification of xenong gas.
[2] K. N. Pushkin, et al. Scintillation light, ionization yield and scintillation decay times in high pressure xenon and xenon methane.

Nuclear Science, IEEE Transactions on, 54(3):744–750, June 2007. ISSN 0018-9499. doi:10.1109/TNS.2007.894815.